N-Aryl-9,10-phenanthreneimines as scaffolds for exploring non-covalent interactions: A structural and computational study

David Farrell,[a] Samuel J. Kingston,[a] Dmitry Tungulin,[a] Stefano Nuzzo,[a] Brendan Twamley,[a]

James A. Platts[b] and Robert J. Baker [a]*

[a] School of Chemistry, University of Dublin, Trinity College, Dublin 2, Ireland

[b] School of Chemistry, Main Building, Cardiff University, Park Place, Cardiff, CF10 3AT, U.K.

Table of content graphic

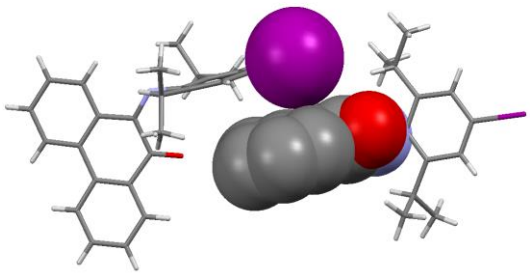

l.p....π favoured

N-Aryl-9,10-phenanthreneimines that feature a halogen on the aryl group show lone pair…π interactions, whilst non-halogenated substituents show π-π stacking.

ABSTRACT. A series of 10-((4-halo-2,6-diisopropylphenyl)imino)phenanthren-9-ones and derivatives of the phenanthrene-9,10-dione ligand have been synthesised and structurally characterised to explore two types of non-covalent interactions, namely the influence of the steric bulk upon the resulting C—H···π and π-stacking interactions and halogen bonding. Selected non-covalent interactions have additionally been analysed by DFT and AIM techniques. No halogen bonding has been observed in these systems, but X lone pair···π, C—H…O=C and C—H···π interactions are the prevalent ones in the halogenated systems. Removal of the steric bulk in N-(2,4,6-trimethylphenyl)-9,10-iminophenanthrenequinone affords different non-covalent interactions, but the C—H···O=C hydrogen bonds are observed. Surprisingly, in N-(2,6-dimethylphenyl)-9,10-iminophenanthrenequinone and N-(phenyl)-9,10-iminophenanthrenequinone these C—H···O=C hydrogen bonds are not observed. However, they are observed in the related 2,6-di-*tert*-butylphenanthrene-9,10-dione. The π-interactions in dimers extracted from the crystal structures have been analysed by DFT and AIM. Spectroscopic investigations are also presented and these show only small perturbations to the O=C—C=N fragment.

Introduction

A number of devices in materials chemistry, such as for applications in organic semiconductors,[1] spintronics,[2] and optoelectronics,[3] rely on π-conjugated organic molecules and polymers and they have generated intensive interest. However to control the important electronic properties the structures of these organic molecules, and in particular the packing, must be well understood. Non-covalent supramolecular interactions therefore become important to study as these can be used to 'tune' the packing, although given the weak nature of these

interactions,[4] this is currently somewhat of an empirical process. Of the multitude of non-covalent interactions reported, aromatic interactions such as C-H…π interactions[5] or π-stacking are important, especially in π-conjugated organic molecules. π-stacking is a much used misnomer and studies to understand the origin of substitution effects have been ongoing for the past two decades. The popular model proposed by Hunter and Sanders,[6] namely π-polarisation, has now been called into question and the model popularised by Wheeler and Houk[7] is consistent with most of the literature. This involves the direct interactions between the C-H/X dipoles of substituted aromatic interactions, which may be attractive or repulsive. A number of recent reviews summarise the current thinking,[8] but it is clear that more experimental data is required. Other non-covalent methods are becoming increasingly recognised include halogen bonding,[9] particularly in supramolecular chemistry and crystal engineering.[10] In some cases these can be more favorable than, and thus compete with (termed *synthon crossover*[11]), or can cooperate with other non-covalent interactions such as hydrogen bonding,[12] lone pair···π[13] or π-stacking.[14] The ability to distinguish between close-packing arrangements and true halogen bonding interactions was first proposed in 1989[15] whereby type I and type II interactions were defined. More recently, the emergence of a quasi-type I and type II have been noted and these individual interactions can be delineated by inspection of the angles such that $0^o \leq |\theta_1-\theta_2| \leq 15^o$ are type I; $15^o \leq |\theta_1-\theta_2| \leq 30^o$ are quasi-type I/type II and $30^o \leq |\theta_1-\theta_2|$ are type II (where θ refers to the two C-X···X angles). Moreover it was found that type II are most favoured with iodine whilst type I are most favored with Cl.[16]

There are few reported structures containing the phenanthere moeity so in this contribution we use it as a platform that contains a plethora of potential interactions *viz*. 'π-π stacking' via the

Wheeler and Houk mechanism, C—H···π; C—X lone pair···π, C—X···H—C and C—X···X—C where we can also control the steric demand of the ligand systems. We specifically look at two types of interactions: (1) those arising from the introduction of a halogen, and (2) those due to steric demands of the ligands. We find that the dominant halogen interaction is a lone pair···π type. DFT and AIM analysis compares the strength of these interactions, which are surprisingly strong (ca. 45 kJ mol^{-1}). Changing the steric bulk of the ligand also changes the nature of the non-covalent interactions and these π-interactions are also characterised computationally.

Results and Discussion

Synthesis and Structural characterisation.

The phenanthrene imines (**1**-**7**) were synthesised according to Scheme 1. The substituted aniline was added to a solution of phenanthrene-9,10-dione along with a catalytic amount of formic acid. This method did not work for aniline, so an alternative method via the $Ph_3As{=}O$ catalysed reaction of phenyl isocyanate and phenanthrene-9,10-dione was used.[17] Workup and purification by column chromatography afforded the desired compounds. Similarly the *tert*-butyl substituted phenanthrene-9,10-dione (**8**) was prepared via a literature method and the three isomers separated by careful column chromatography; we could not grow crystals suitable for X-ray diffraction for the other two isomers so these are not included in our study. Finally we attempted the reaction with the very bulky 2,4,6-tri*tert*butylaniline, but no reaction occurred, even after prolonged reflux. Crystals of all were obtained by the slow evaporation of chloroform, Bu_2O (**5**) or hexane (**7**) solutions. The discussion will firstly focus on the molecular structures, followed by the packing arrangements and the description of the non-covalent interactions present.

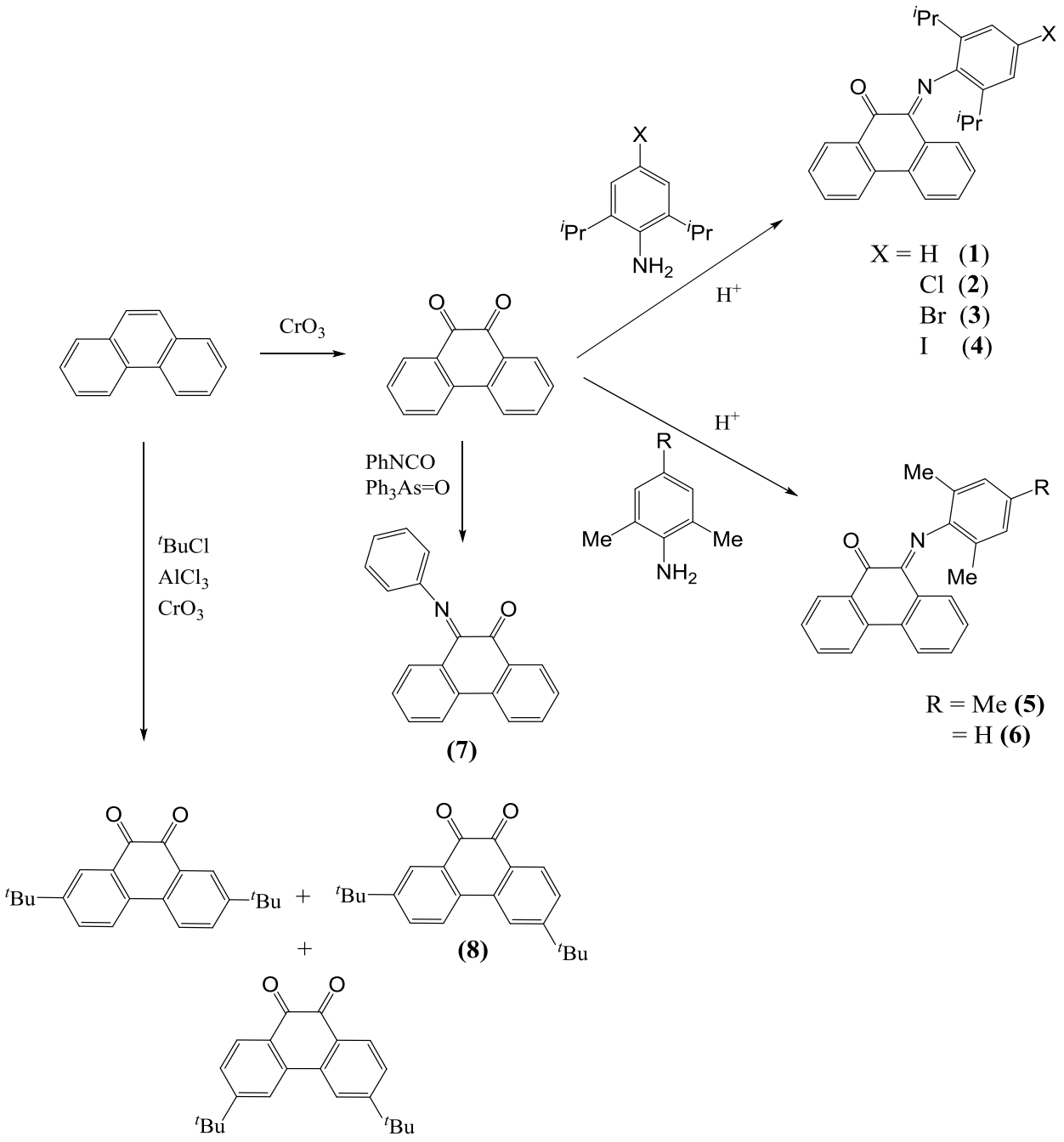

Scheme 1. Synthesis of compounds described in this work.

1 suffers from whole molecule disorder and we refrain from discussing the metric parameters; the structure is shown in Figure S1. The molecular structures of **2, 3, 6, 7** and **8** are representative of the library of compounds and shown in Figures 1-5 whilst **4** and **5** are shown in Figures S3-S4 respectively. In the series **2-7** the metric parameters of the phenanthrene backbone do not change and the C—C, C=N and C=O bond lengths are also essentially identical (Table 1). The most noticeable difference is the planarity of the phenanthrene backbones which are disrupted in **2** and **6** and to a much lesser extent in **3**; while **4, 5** and **7** are flat. **2** has two molecules in the asymmetric unit; whilst the bond lengths in **2a** and **2b** are identical, remarkably the planarity of the phenanthrene backbones differ. In molecule **2a** the torsion angles C(7)—(C8)—C(9)—C(10) = 6.6(4)^{o} and O(1)—C(2)—C(15)—N(16) = 16.2(4)^{o} whilst in molecule **2b** the torsion angles C(35)—(C36)—C(37)—C(38) = 11.5(4)^{o} and O(29)—C(30)—C(43)—N(44) = 29.6(4)^{o}. A survey of the Cambridge database shows that the median of the C-C-C-C torsion angle = 2.999^{o} and of the X-C-C-X = 2.882^{o} (X = any atom); deviations are generally due to steric effects (Figure S5). **7** has two molecules in the unit cell, one of which is disordered, but the metric parameters are identical. In addition the C=O and C=N are significantly out of the plane of the phenanthrene unit.

Table 1. Selected structural parameters in the structures of **2-8** (in Å and °).

	C=O	C=N	C-C	C-C-C-C	N-C-C-O	C=N oop[a]	C=O oop[a]	α[b]	β[b]
2a	1.216(3)	1.282(3)	1.526(3)	6.6(4)	16.2(4)	-0.429	0.375	-	-
2b	1.220(3)	1.275(3)	1.520(3)	11.5(4)	29.6(4)	-1.013	0.375	70	112
3	1.216(2)	1.279(2)	1.519(2)	5.2(2)	15.2(2)	-0.320	0.226	82	85
4	1.208(5)	1.280(5)	1.519(6)	2.3(6)	8.8(6)	-0.179	0.142	89	79
5	1.218(3)	1.280(3)	1.520(2)	2.1(3)	8.6(3)	-0.193	0.123	-	-
6	1.218(3)	1.278(4)	1.517(4)	9.11(4)	29.1(4)	-0.546	0.787	-	-
7a[c]	1.215(7)	1.273(8)	1.506(9)	3.3(9)	13.7(10)	-0.170	0.464	-	-
8	1.215(2) 1.220(2)	-	1.541(2)	7.1(2)	6.3(2)	-	0	-	-

a o.o.p = distance out of the plane of the phenanthrene backbone (Å)

b intermolecular contacts α is the angle between the plane of the ring, centroid and X,[13d] whilst β = C-X···centroid angle.

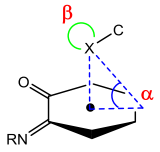

c = There are two molecules in the asymmetric unit of which one is disordered. Only dimensions from the ordered molecule (7a) are reported.

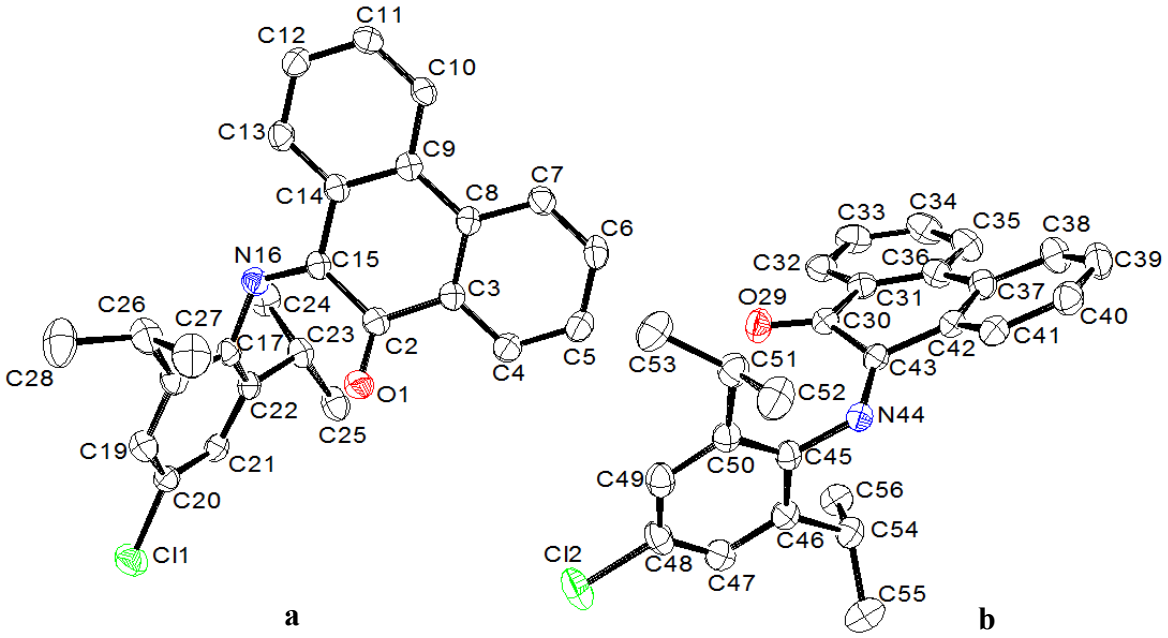

Figure 1. Molecular structure of **2** with atomic displacement parameters shown at 50% probability. The two molecules are labelled as **2a** and **2b** in the text. Hydrogen atoms omitted for clarity.

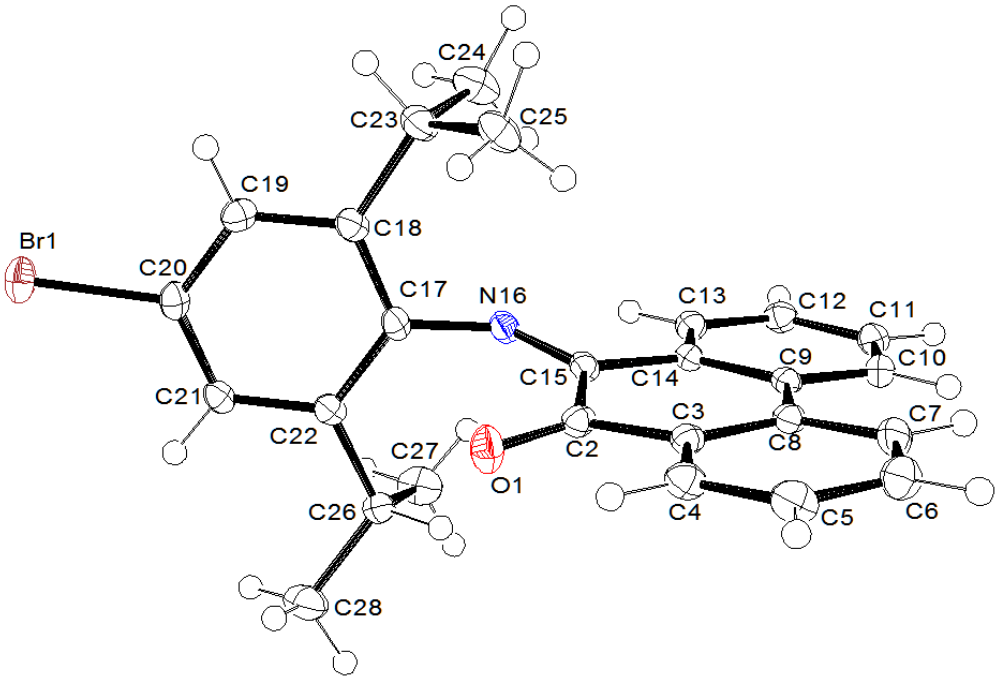

Figure 2. Molecular structure of **3** with atomic displacement parameters shown at 50% probability.

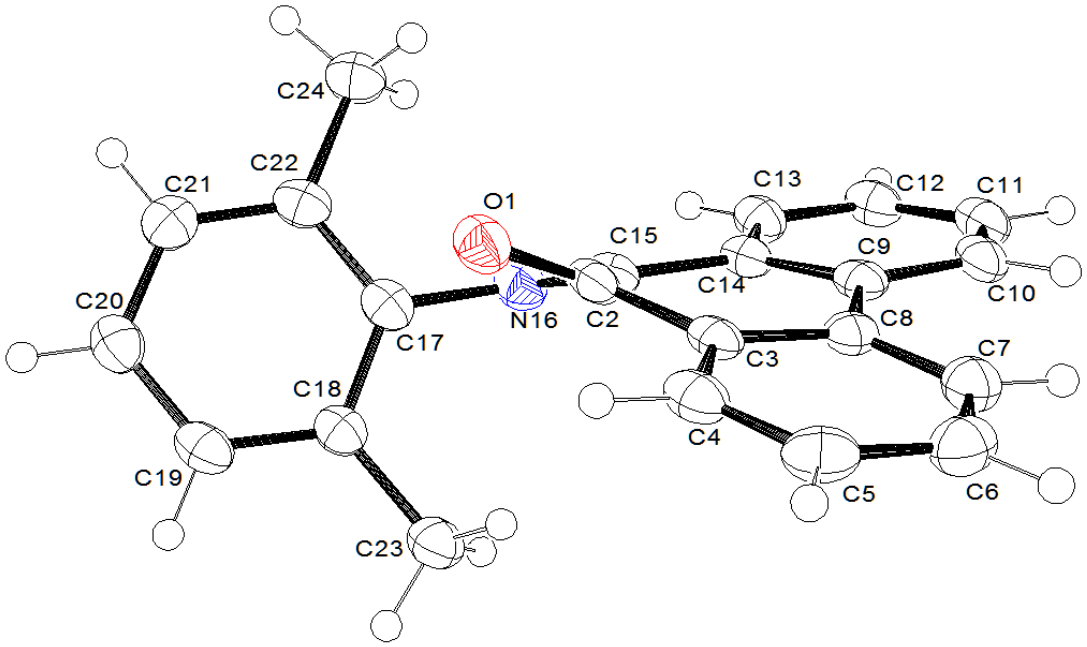

Figure 3. Molecular structure of **6** with thermal displacement shown at 50% probability.

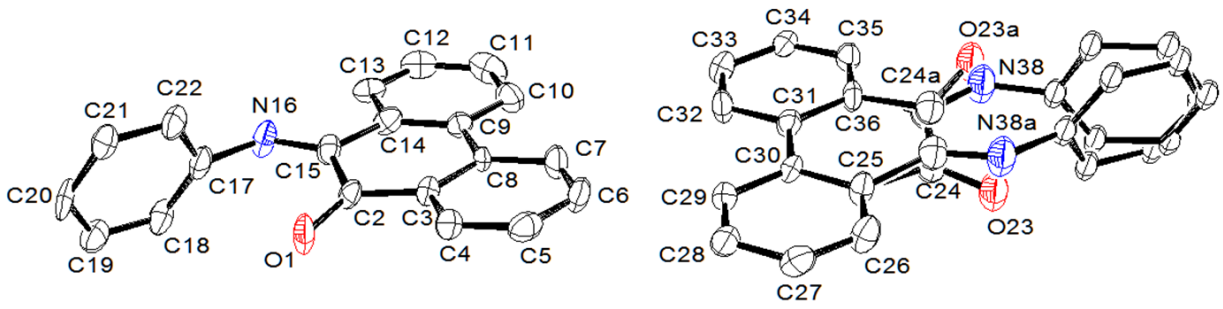

a b

Figure 4. Major (7a: 82%) and minor (7b: 18%) disordered moiety of **7** with thermal displacement shown at 50% probability. Hydrogen atoms omitted for clarity.

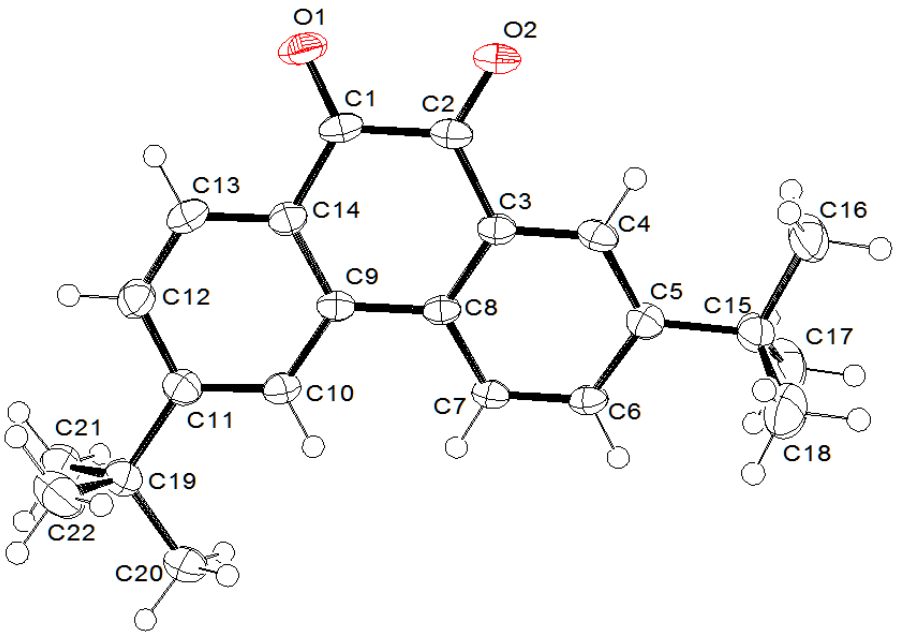

Figure 5. Molecular structure of **8** with thermal displacement shown at 50% probability.

In the structure of **8**, the C(1)—C(2) bond length of 1.541(2) Å and the C=O bond lengths of 1.220(2) and 1.215(2) are typical for phenanthrene-9,10-diones, e.g. 1.52(3) to 1.524(5) Å for the C—C and 1.207(6)-1.25(2) Å for the C=O in the different polymorphs of phenanthrene-9,10-dione.[18] There is a relatively small deviation from planarity (C(7)—C(8)—C(9)—C(10) = 7.07(2) º); steric bulk at the C(7) and C(10) positions invokes a bigger bending e.g. 39.9º in 2,4,5,7-tetramethyl-9,10-phenanthroquinone.[19]

Packing and intermolecular interactions in 2-4.

We first focus on the halogen series. In the structures of **2-4** there are no C—X···O=C or X···X interactions present, but some identical interactions are observed (Figure 6). In **2** there are a number of C—H···O interactions[20] between H(5) and H(6) (hydrogens are in the calculated positions in all structures; $d_{C...O}$ = 3.293(3) and 3.279(3) Å) and C—H···N interactions involving N(44) and H(7) and H(10) ($d_{C...N}$ = 3.633(11) and 3.618(8) Å) (Figure 6a); if **2** is recrystallized from DMF, the same structure is formed, indicating that the crystal packing interactions are reproducible in different solvents. In contrast, in **3** and **4** the C—H···O are from H(10) and H(11) (**3**: $d_{C...O}$ = 3.123(4) and 3.081(4) Å; **4**: $d_{C...O}$ = 3.108(5) and 3.117(6) Å) and no C—H···N interactions are present (Figure 6c for **3**; **4** is identical). A C—H···π interaction from a phenanthrene H to the X-substituted aryl group ($d_{C—H...cent}$ = 2.564 Å) is present in **2** (Figure 6a), whilst in **3** and **4** there is also longer one from an isopropyl hydrogen to the phenanthrene (**3**: $d_{C—H...cent}$ = 2.576 and 3.160 Å; **4**: $d_{C—H...cent}$ = 2.552 and 3.126 Å; Figure 6b). In **2a,** there are phenanthrene groups not involved in a l.p.···π interactions but are close to another Cl atom – inspection of the angles show that this is a type I interaction. There is a short contact of 3.238 Å between the C—Cl and the centroid of an adjacent phenanthrene ring which has the larger deviation from planarity (**2b**) and shown in Figure 6b. This lone pair···π interaction is of a semi-localized type according to the scheme developed by Shishkin,[21] and within the sum of van der Waals radii (C···Cl = 3.45 Å). In **3** and **4** this lone pair···π interaction (**3**: 3.396(8) Å; **4**: 3.569(7) Å; Figure 8d) is a delocalized interaction[21] where and inspection of the α and β angles shows that the heavier halogens move close to the centre of the ring (Table 1). Both are within the van der Waals radii (3.55 Å for C···Br and 3.68 Å for C···I). However, a recent high level theoretical

study has shown that in R—Br···π interactions with benzene (R = H, HC≡C and NC), it is only the distance that influences the strength of the interactions and not the angles.[22] The closest Br···Br and I···I distances are 4.370(6) and 4.125(6) Å respectively and thus outside the sum of the van der Waals radii. The second form of weak hydrogen bonds are X···H—C_{sp2} (**2**: $d_{C\cdots Cl}$ = 3.781(3) Å; **3**: $d_{C\cdots Br}$ = 3. 800(4) Å) from a phenanthrene hydrogen in **2** and an isopropyl hydrogen in **3**; in **4** there are no C—H···I contacts within the sum of the van der Waals radii. There are no obvious π-π stacking interactions in **2-4**, presumably due to the increased steric demand of the halogen substituents.

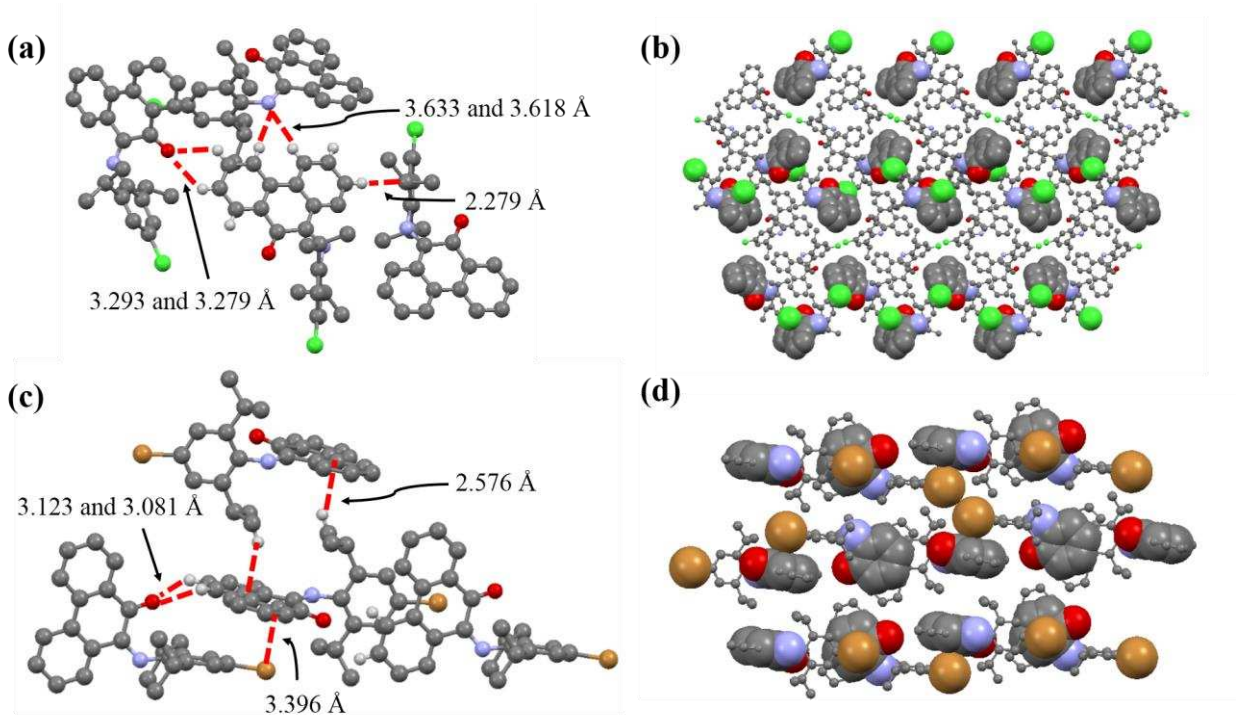

Figure 6. **(a)** View of **2** highlighting the non-covalent interactions; **(b)** packing of **2** as viewed along the crystallographic *c*-axis; **(c)** view of **3** highlighting the non-covalent interactions; (d) packing of **3** as viewed along the crystallographic *b*-axis. Colour code: Cl – green; Br – brown; only hydrogen atoms involved in hydrogen bonds are shown, others are omitted for clarity.

DFT and AIM calculations on lone pair···π interactions.

In order to ascertain whether the lone pair···π interaction is simply due to crystal packing, we utilized a DFT and AIM approach. Dimers exhibiting a range of intermolecular interactions were extracted from the crystal structure of **4**, and counterpoise-corrected binding energies calculated with M06-2X with both Def2TZVP and Def2SVP basis sets. The dimers are bound by -43.9 and -43.6 kJ mol^{-1}, respectively. We also included a dispersion-corrected functional (B97D), which gives a binding energy of -58 kJ mol^{-1}. Given the excellent agreement between the basis sets, the computationally smaller Def2SVP basis can be used to give qualitative data for comparison between our small library of compounds (the dimers can be seen in Figures S28-S36). While dimers may not entirely reproduce the overall crystal environment, this approach allows us to interrogate individual types of interaction, and also to compare observed and hypothetical interaction modes on an equal footing.

The isostructural dimer of **3** containing X···π contacts are bound by -45.5 mol^{-1}. A hypothetical dimer of **2**, constructed by replacement of Br by Cl followed by optimization of the position of Cl, is bound by -42.2 kJ mol^{-1} and so almost identical to those for **3** and **4.** In contrast, the real dimers of **2** extracted from the crystal structure are much more weakly bound: the dimer containing Cl···π contacts is bound by -22.3 kJ mol^{-1}, while that containing Cl···Cl contact is predicted to be unbound (binding energy = +2.1 kJ mol^{-1} after counterpoise correction), in agreement with the assignment of a type I interaction. It is important to note that this is the total energy of the interactions between the dimers, and not of individual components, but lone pair···π interactions, in cooperation with other non-covalent interactions are energetically significant; this has been noted in previous examples.[8a],[23]

The molecular electrostatic potentials have been calculated for the monomeric units in **2**-**4**. Figure 7 shows the results for **4**, but all are similar (Figures S6 and S7 show the plots for **2** and **3**). There is a σ-hole on the iodine atom but is small; for **2** and **3** this is not observed and this is likely due to the differences in electronegativity of the halogen atom.[24] A small π-hole, defined as a positive region, on the central phenanthrene ring (**3** = 2.2 x 10^{-2} a.u.; **4** = 2.9 x 10^{-2} a.u.) is evident, corresponding to the lone pair···π interaction; in the plot of **2** this is absent and corroborates the differences in binding energies. The aromatic hydrogens are slightly δ^+, possibly due to the polarizing effect of the carbonyl function, and could explain the prevalence of the C—H···O hydrogen bonds.[25]

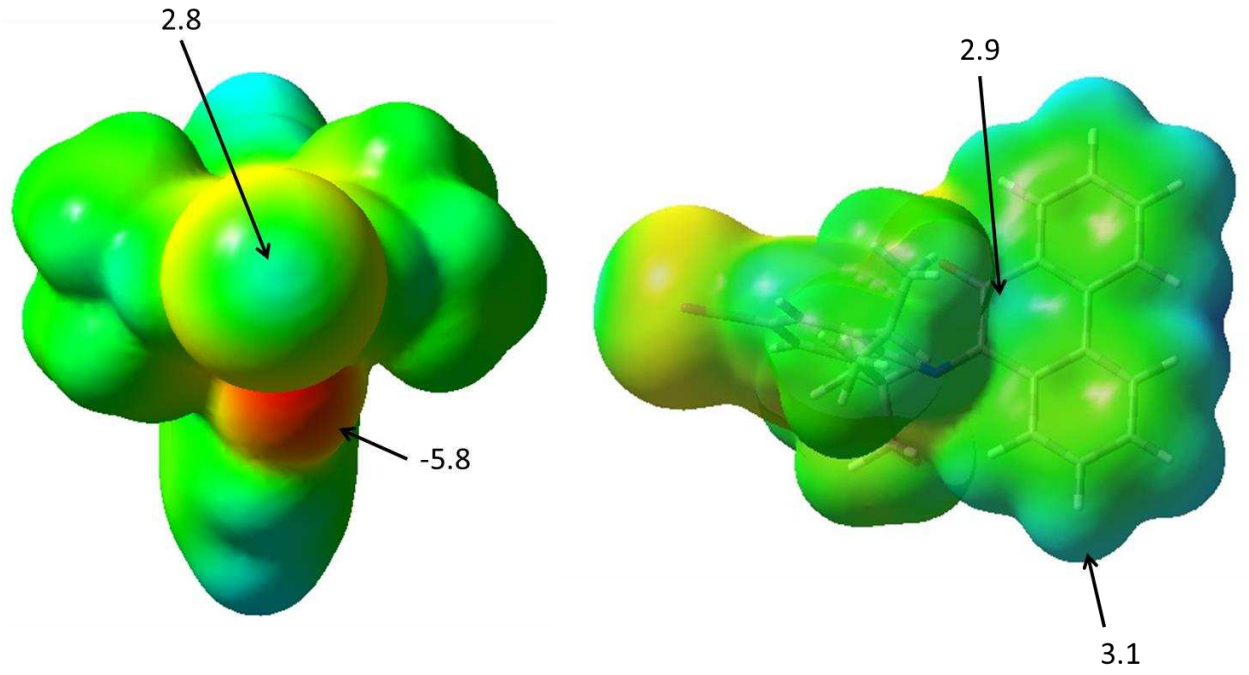

Figure 7. Molecular Electrostatic Potential of **4** (numerical values are x 10^{-2} a.u; colour: blue = 6.0 x 10^{-2} to red = -6.0 x 10^{-2} a.u.).

AIM analysis showed multiple bond paths corresponding to intermolecular interactions, as shown in Figure 8 and Table 2. Two X···π bond paths are present, along with one C—H···X path. A further three π···π contacts and one C—H···π are predicted, along with two C—H···O contacts. The value of the electron density at the bond critical point, ρ_{bcp}, is widely used as an estimate of the strength of contacts: largest values are observed for C—H···O, followed by X···π with C—H···π and π···π contacts predicted to be the weakest. The literature is replete with computational studies of lone pair···π interactions, and the electron density at the bcp is similar to that calculated for a variety of electron rich or electron poor arenes and lone pairs originating from oxygen or nitrogen donors.[26]

Table 2. Calculated electron density (in a.u.) at bcps in the dimers extracted from **2-4**.

Compound	C—H···O	X···π	C—H···X	C—H···π	π···π	X···X
2 hypothetical	0.008, 0.010	0.006, 0.007	0.006	0.006	0.005 x2, 0.006	
2 X···X						0.008
2 X···π		0.010	0.005	0.003, 0.004 x2		
3	0.008, 0.009	0.007 x2	0.009	0.006 x2	0.005 x2, 0.006	
4	0.009, 0.010	0.006 x2	0.007	0.004	0.004, 0.005 x2	

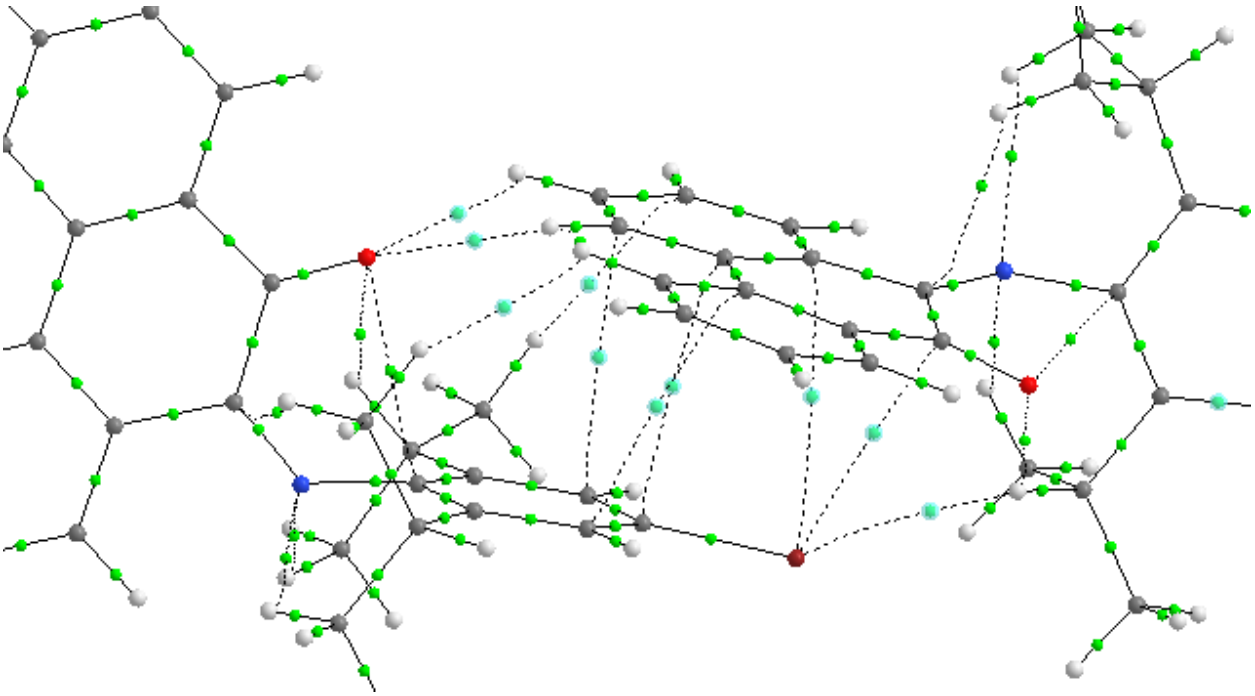

Figure 8. AIM properties of **3** displaying intermolecular bond paths as dotted lines.

Packing and intermolecular interactions in 1, 5-8.

Compounds **1**, **5, 6** and **7** allows us to probe the relative stability of the non-covalent interactions when the steric demands of the ortho-groups are changed, and perhaps comment on the potential of π-interactions. The packing of **1** is shown in Figure S2; there are only C—H···π interactions present between a phenanthrene hydrogen and the centroid of the aryl ring ($d_{C\cdots cent}$ = 2.570 Å) in this structure. The packing of **5** (Figure 9a) has no C—H···π interactions and two C—H···O interactions ($d_{C\cdots O}$ = 3.370(3) and 3.493(3) Å), which forms chains. There are also 'π-π stacking' between two phenanthrene rings ($d_{cent\cdots cent}$ = 3.622 Å) that stack in a head to tail fashion. However in **6** (Figure 9b), where only one methyl group in the para-position has been removed, the C—H···O hydrogen bond is no longer present. Instead, the prevalent interaction in **6** is 'π-π

stacking' between two phenanthrene rings ($d_{cent\ldots cent}$ = 3.929 Å), longer than that found in **5**. There are also weak C—H···N hydrogen bonds ($d_{C\ldots N}$ = 3.606(14) Å), comparable to that observed in **2a**. **7** (Figure 9c) has a different packing where C—H…π interactions dominate whereby hydrogens (H12 and H5) on the phenanthrene backbone and the phenyl ring of the disordered imine are involved and extend along the crystallographic *b*-axis. 'π-π stacking' between two phenanthrene rings ($d_{cent\ldots cent}$ = 3.803 Å) and C—H…O interactions ($d_{C\ldots O}$ = 3.218(8) Å) are present, but the latter involves hydrogens on C(13) and not the same as that observed in **2**-**4**. Therefore as the steric bulk is reduced around the ortho-positions from ^{i}Pr to Me to H the propensity for 'π-π stacking' increases, as might be expected. Surprisingly however there is a difference between the mesityl and xylyl substituents, and we are not sure of an explanation for this.

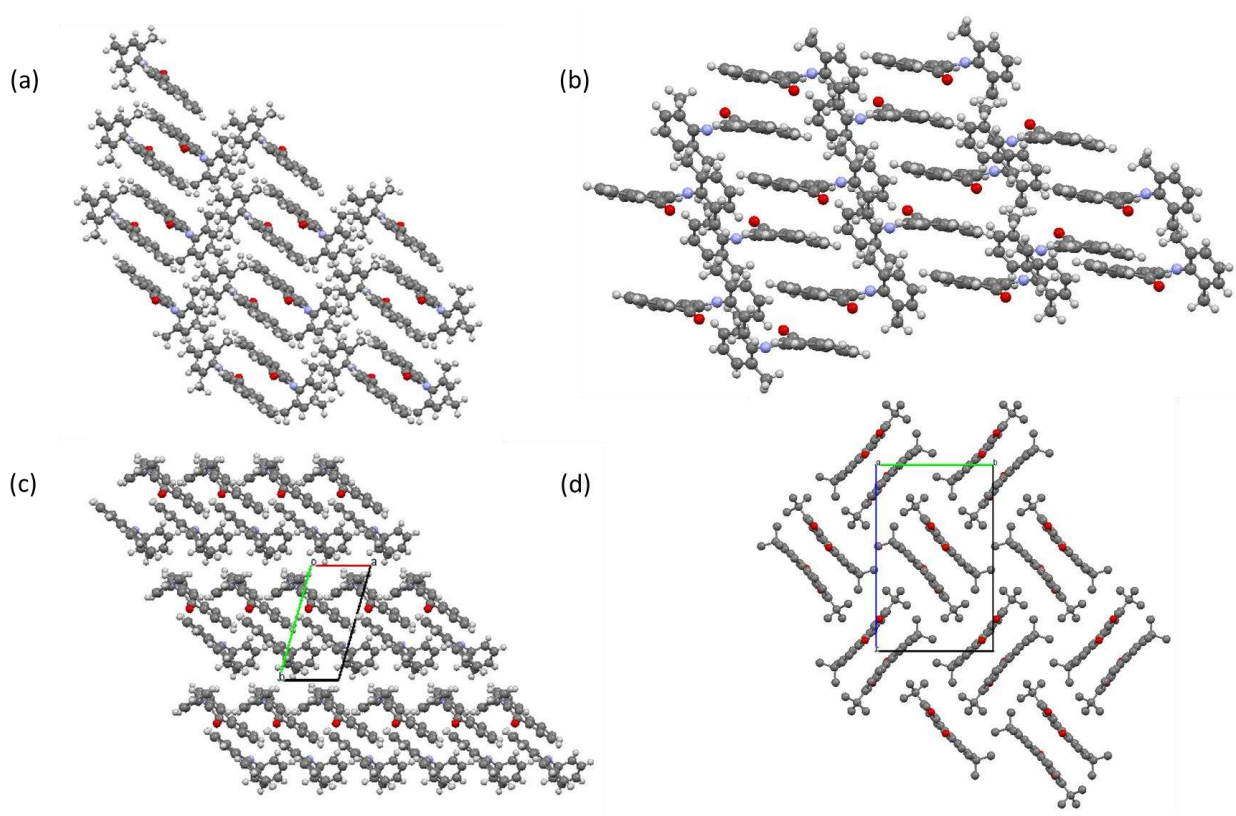

Figure 9. Packing of (a) **5** and (b) **6** viewed along the crystallographic *b*-axis; (c) **7** viewed along the crystallographic *c*-axis; (d) **8** viewed along the crystallographic *a*-axis.

In order to further analyse the influence of the steric bulk of the ligand, the structure of **8** (Figure 9d) is useful as the steric bulk is closer to the seemingly principal C—H···O interactions. **8** is built up of chains of phenanthrene-9,10-diones hydrogen bonded {$d_{C\cdots O}$ = 3.243(2) and 3.392(2) Å} along the *c*-axis and a head-to-tail 'π-π stacking' between the two central rings ($d_{cent\cdots cent}$ = 3.759 Å) and in the outer rings ($d_{cent\cdots cent}$ = 3.772 Å), along with C—H···π interactions.

DFT and AIM calculations on 5-8.

In order to examine the π-interactions in these species we have used the same computational methodology as described above (M06-2x/Def2SVP level) and in our previous work.[27] The binding energies of the dimers extracted from the crystal structures are -52.94 kJ mol^{-1} for **5**, -48.54 kJ mol^{-1} for **6**, -36.53 kJ mol^{-1} for **7** and -74.45 kJ mol^{-1} for **8**. A possible explanation for the interactions comes from the molecular electrostatic potentials shown in Figure 10 for **5** and **8** (**6** and **7** are similar and are shown in Figure S8 and S9). From this analysis the hydrogen atoms on the phenanthrene are polarised due to the C=O and C=N (for **5**-**7**) electron withdrawing groups, but as the prevalent interaction is a head to tail stacking, it follows that the positively polarised hydrogens are preferentially interacting with the negatively polarised carbonyl function. This is consistent with the direct interactions proposed by the Wheeler and Houk mechanism for non-covalent π-interactions.

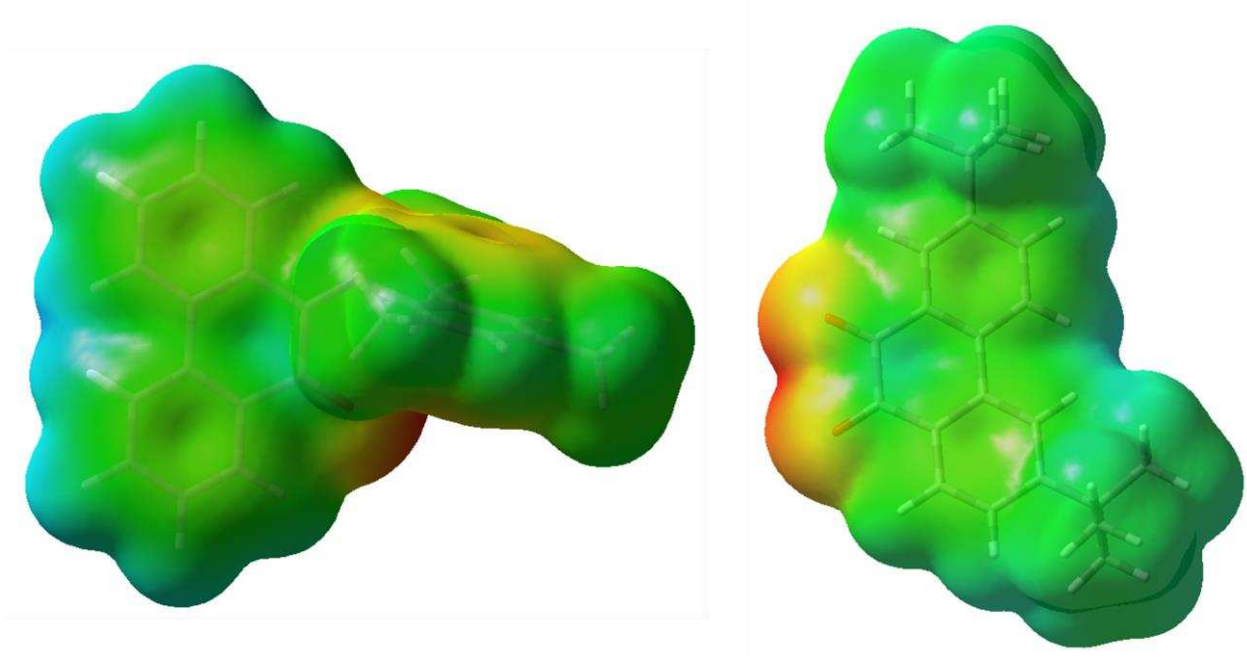

Figure 10. Molecular Electrostatic Potential of **5** (left; colour: blue = 6.7 x 10^{-2} to red = -6. 7 x 10^{-2} a.u.) and **8** (right; colour: blue = 8.0 x 10^{-2} to red = -8.0 x 10^{-2} a.u.).

AIM analysis of **5-8** showed multiple bond paths corresponding to intermolecular interactions, as shown in Figure 11 and Table 3. There are a number of π···π contacts, C—H···π and C—H···O contacts in this series. Examination of the electron density at the bond critical point, ρ_{bcp}, shows the trend that the π···π contacts are stronger than C—H···π. Moreover **7** appears to report the weakest binding, in line with the binding energies; **8** on the other hand has the most stabilisation from π···π contacts.

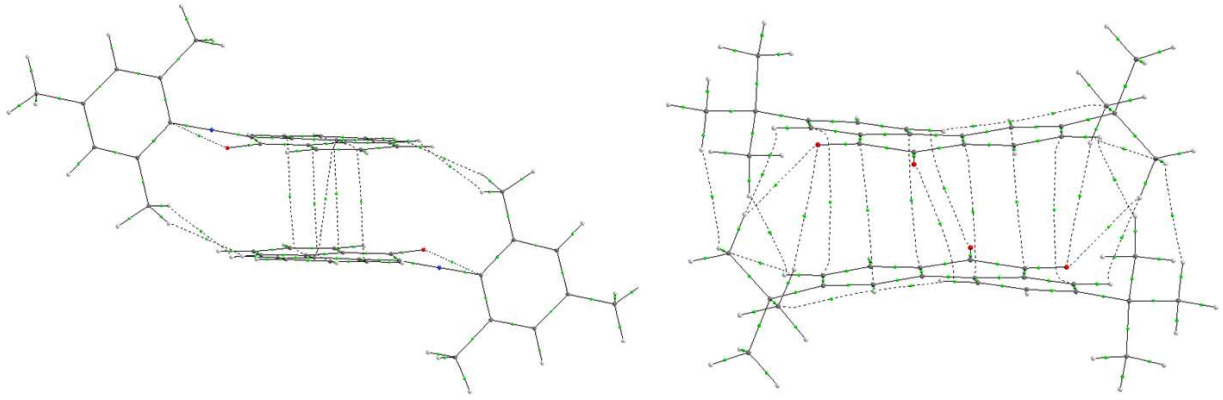

Figure 11. AIM properties of **5** (left) and **8** (right) displaying intermolecular bond paths as dotted lines.

Table 3. Calculated electron density (in a.u.) at bcps in the dimers extracted from **5-8**.

Compound	C—H···O	O···π	C—H···π	π···π
5			0.006 x 2 0.005 x 2	0.007 x 2 0.006 x 3
6			0.002 x 2	0.006 x 2 0.005 0.004 x 2
7	0.007 x 2			0.006 x 2
8		0.004 x 2	0.002 x 4	0.007 x 2 0.004 x 4

Hirshfeld analysis

To extend our study on the different packing arrangements we have used Hirshfeld analysis.[28] The results of the fingerprint analysis for the lone pair···π interactions in **2-4** are shown in Figure

12. It is clear from this that the dominant interaction is H···H, but C···H (i.e. C—H···π) are significant. X···lone pair interactions are small but clearly observed, particularly in the plot of the shape index. The C—H···π interaction is the largest for **7** according to this analysis.

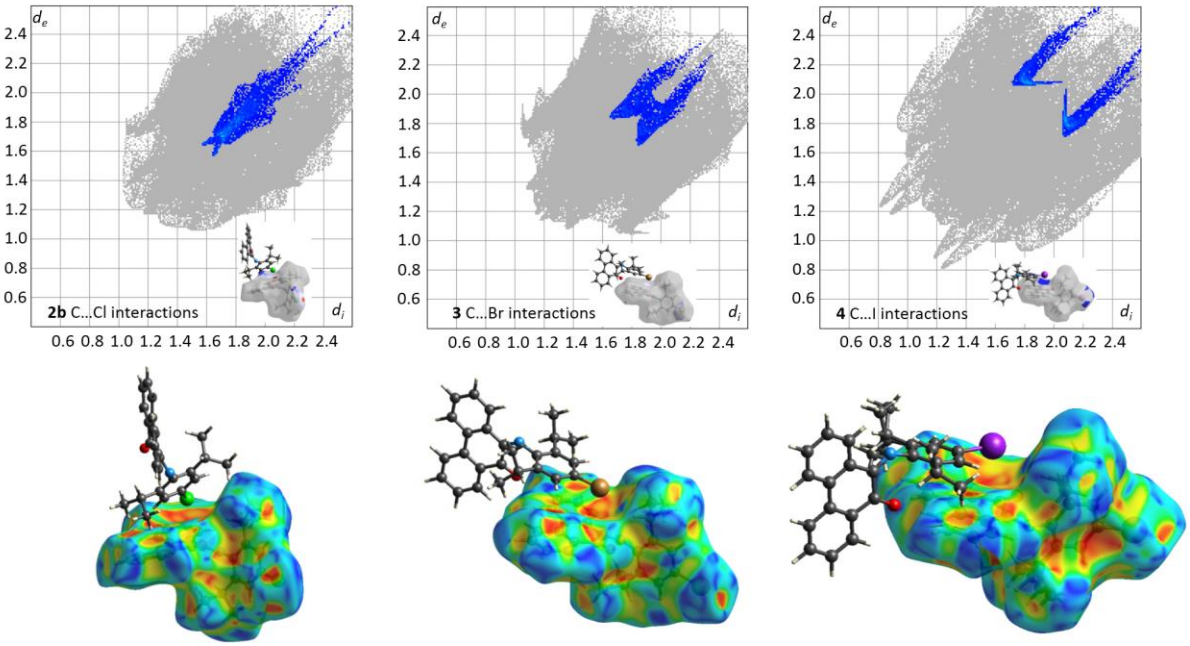

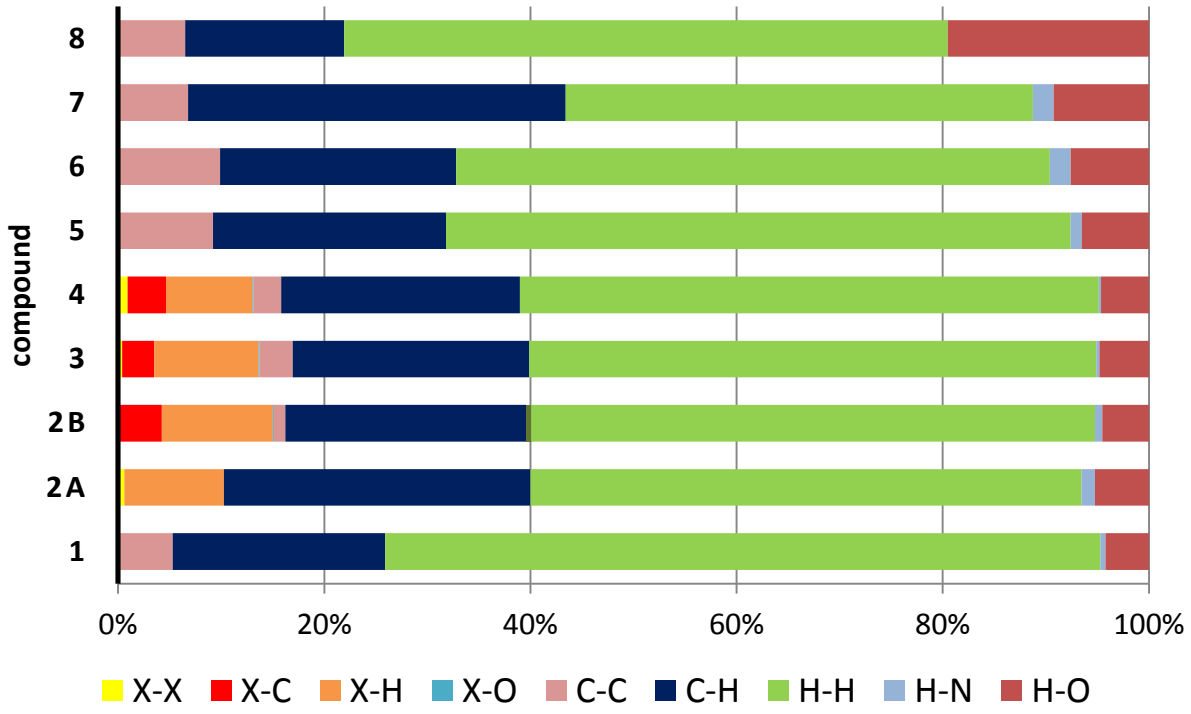

Figure 12. (top) Fingerprint plots of **2b**, **3** and **4** displaying the X···C interactions (d_{norm} plotted at -0.161 to 1.605), (middle) the shape index (plotted at -1 to +1) and (bottom) the quantitative analysis of the Hirshfeld surfaces for **1**-**8**.

Further Reactivity Studies

Given that no XB bonding was observed in **2**-**4** we next tried a number of co-crystallization experiments to see if we could engineer XB. It is known that asymmetric XB typically goes via Type II interactions,[9] so we co-crystallized a mixture of **2** and **4**; the resulting structure, **9**, (Figure S10) showed a disordered structure with a statistical mixture of chloro and iodo substituents, but the packing interactions were of the iodo type. Next we tried the reactions of **3** with Br_2 and **4** with ICl and I_2, for which we only obtained crystals of the latter. The structure showed that the iodide had been partially lost and the structure (**10)** was a disordered mixture of

4 and **1** (Figure S11). We are unsure of the mechanism of this transformation, but it could be that the I_2 used contained a small amount of impurities such as HI. Further details can be found in the ESI.

Spectroscopic characterization.

Infrared and UV-vis spectroscopy were utilized to characterize these compounds, and the pertinent parameters are recorded in Table 4. The C=O and C=N bond stretching frequencies in the infrared spectra of crushed single crystals are barely perturbed suggesting that both the electronic influences of the para-substituent are not particularly strong and the hydrogen bond interactions discussed above are weak.

Table 4. Spectroscopic properties of phenanthrene imines **1-7, 8** and phenanthrene-9,10-dione.

			λ_{max} (nm) (ε, M^{-1} cm^{-1})		
Compound	**ν(C=O) (cm^{-1})**	**ν(C=N) (cm^{-1})**	**π-π***	**π-π***	**n-π***
Phenanthrene-9,10-dione	1674	-	319 (3805)	-	412 (1453)
1	1679	1589	315 (1488)	390 (530)	587 (96)
2	1677	1592	314 (2367)	380 (733)	583 (160)
3	1681	1592	318 (3253)	389 (869)	574 (199)

4	1679	1591	313 (3557)	385 (1389)	581 (285)
5	1675	1590	313 (2150)	378 (800)	599 (162)
6	1677	1591	314 (4954)	388 (1604)	575 (302)
7	1647	1591	312 (4497)	-	540 (530)
8	1675	-	325 (2034)	-	426 (522)

The UV-vis spectra of the compounds in CH_3CN are shown in Figure 13. In the series **1**-**8** a broad, weak band at ca. 600 nm appears upon substitution of the aryl ring. This has been assigned to C=O and C=N n-π* transitions, whereby the intensity variations likely due to deviations from non-planarity of the carbonyl and imino fragments.[29] The molar extinction coefficients of the bands at 390 nm and 315 nm, the π-π* transitions within the phenanthrene ring, increase upon halogen substitution from **1**-**4**. Similarly the small shifts in intensity and extinction coefficients of **9** compared to the unsubstituted phenanthrene-9,10-dione are likely due to the structural variability caused by the increasing steric bulk and the deviations from planarity of the imino and carbonyl groups. Thus the UV-vis data suggest generally small perturbations to the electronic structure due to the structural variations.

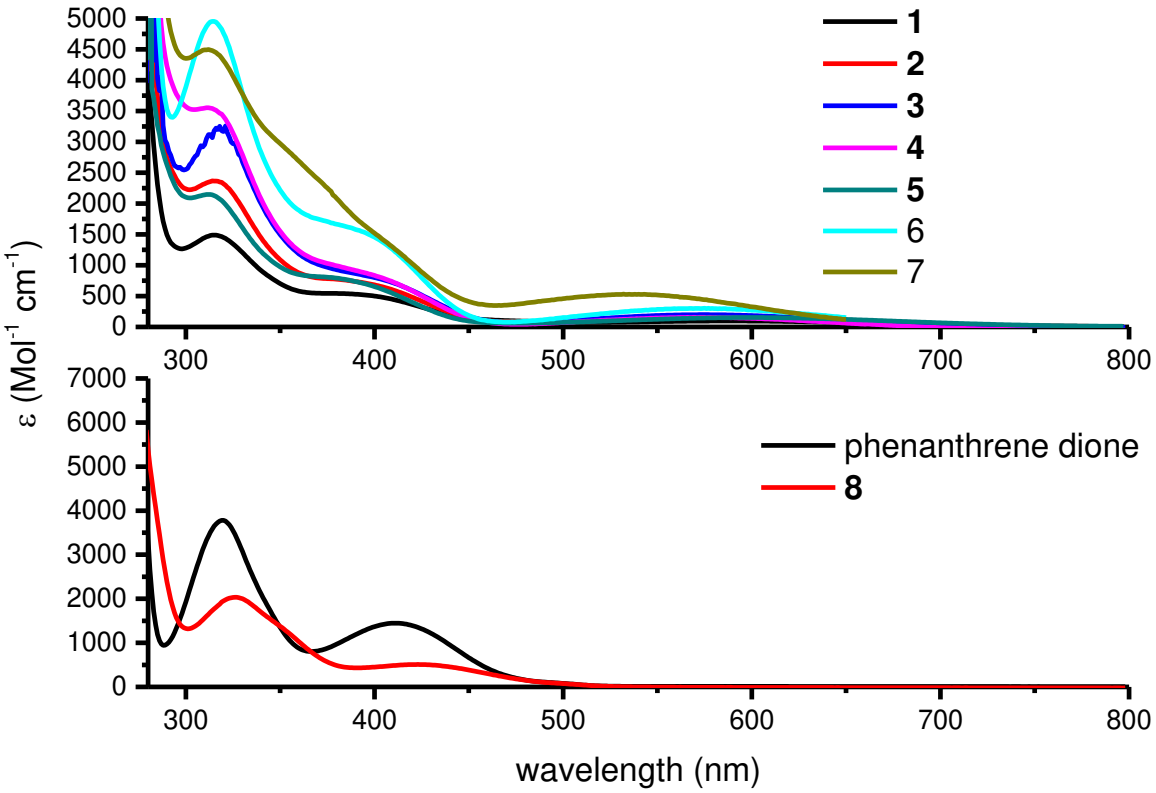

Figure 13. Electronic absorption spectra of the compounds **1-8** in CH_3CN solution (concentration ≈ 1 x 10^{-5} M).

Conclusions

In summary, we have structurally characterised a number of examples based on a phenanthrene core and shown that lone pair···π interactions are the dominant halogen type interaction and a computational study shows that these are stabilizing and of the same order of magnitude as interactions from lone pairs originating from oxygen or nitrogen donor atoms. However the most important interaction appears to be a weak hydrogen bond between the C—H of a phenanthrene and the carbonyl oxygen. Inspection of the molecular electrostatic potential shows that the

aromatic hydrogen atoms are polarized, probably due to the C=O and C=N function on the opposite side of the ring, which can account for this interaction. The steric bulk of the imino aryl group has been evaluated and as the steric requirements are reduced then 'π-π stacking' and eventually C—H…π interactions dominate. We posit that the molecular electrostatic potentials of these compounds are in line with the Wheeler and Houk mechanism for non-covalent π-interactions.

Experimental

^{1}H, and ^{13}C{^{1}H} spectra were recorded on a Bruker AV400 spectrometer operating at 400.23 MHz and 155.54 MHz respectively, or a Bruker Avance II 600 NMR with a TCI cryoprobe spectrometer operating at 150.92 MHz (^{13}C) and were referenced to the residual ^{1}H and ^{13}C resonances of the solvent used. IR spectra were recorded on a Perkin Elmer Spectrum One spectrometer with attenuated total reflectance (ATR) accessory. Mass spectra were measured on a MALDI QTOF Premier MS system. UV-vis measurements were made on a Perkin Elmer Lambda 1050 spectrophotometer, using fused silica cells with a path length of 1 cm. 4-X-2,6-diisopropylaniline (X = Cl,[30] Br,[31] I[32]), N-(phenyl)-9,10-iminophenanthrenequinone[17] and 2,6-di-*tert*-butyl-9,10-phenanthrenequinone[33] were prepared according to literature procedures. All other chemicals and solvents were obtained from commercial sources and used as received.

X-ray crystallography: data were measured on either a Bruker SMART Apex Duo Kappa (**1-4**, **8**) or a Bruker D8 Quest Eco (**5**, **6**, **7**, **9**, **10**) diffractometer at 100 K using an Oxford Cobra (Duo) or Cryostream (Eco) with samples mounted on a MiTeGen microloop. Bruker APEX software[34] was used to collect and reduce data and determine the space group. Absorption

corrections were applied using SADABS 2014.[35] Structures were solved with the XT structure solution program[36] using Intrinsic Phasing and refined with the XL refinement package[37] using Least Squares minimisation in Olex2.[38] All non-hydrogen atoms were refined anisotropically. Hydrogen atoms were assigned to calculated positions using a riding model with appropriately fixed isotropic thermal parameters. Crystal data, details of data collections and refinement are given in Table 5 and Table S1 for **9** and **10**. Further refinement details are given in the Supporting Information. CCDC 1504190-1504197 and 1520301-1520302 contains the supplementary crystallographic data for this paper. These data can be obtained free of charge from The Cambridge Crystallographic Data Centre via www.ccdc.cam.ac.uk/data_request/cif.

DFT calculations were carried out in Gaussian09[39] with the meta-hybrid M06-2X functional[40] recommended for study of non-covalent interactions and def2-SVP basis set.[41] All calculations of interaction energy used the counterpoise method to account for basis set superposition error,[42] and positions of hydrogen nuclei normalised to optimal positions by partial geometry optimisation with all heavy-atom positions fixed. Converged molecular orbitals were obtained from these calculations and used for topological analysis of the resulting electron density using the AIMAll package.[43]

General Synthesis of mono substituted iminophenanthrenequinones.

Phenanthrenequinone (1 eq.) and the appropriate aryl amine (ca. 1.2 eq.) were dissolved in methanol. To this reaction catalytic amounts of formic acid were added and refluxed for 12 h. The reaction was diluted in hexane and the solvent evaporated. The crude sample was eluted

from silica gel with an ethyl acetate/hexane solution (0 – 3 % ethyl acetate in hexane). The desired fractions were concentrated to yield the pure product. The numbering schemes for the NMR spectroscopic assignments are shown in Figure 14.

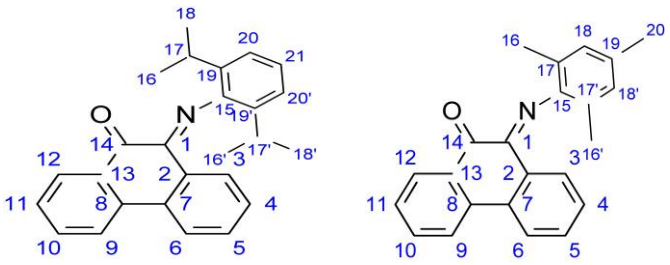

Figure 14. Numbering scheme for NMR spectroscopic data

N-(2,6-diisopropylphenyl)-9,10-iminophenanthrenequinone (1).

Phenanthrenequinone (0.4172 g, 2.00 mmol) and 2,6-diisopropylaniline (0.75 cm^3, 3.98 mmol) were reacted according to the method to yield (**1**) as a dark green solid (0.4965 g, 68 %). M.Pt.: 142 – 145 ºC; υ (cm^{-1}): 3072 (w), 2960 (s), 2864 (m), 1679 (s, C=O), 1589 (s, C=N), 1478 (w), 1461 (w), 1450 (s), 1434 (m), 1294 (s), 1281 (s), 1254 (s), 1232 (s), 963 (w), 937 (m), 882 (w), 868 (w), 830 (w), 807 (w), 797 (m), 782 (m), 773 (m), 754 (s), 721 (s), 704 (w); ^{1}H NMR ($CDCl_3$) δ = 1.13 (6 H, d, J = 6.4 Hz, CH_3 – 16 and 16'), 1.24 (6 H, d, J = 6.4 Hz, CH_3 – 18 and 18'), 2.74 (2 H, m, CH – 17 and 17'), 7.20 (1 H, m, CH – 21), 7.27 (2 H, d, J = 7.6 Hz, CH – 20 and 20'), 7.48 (1 H, m, CH – 4), 7.60 (1 H, t, J = 7.2 Hz, CH – 5), 7.72 (1 H, t, J = 7.6 Hz, CH – 11), 7.78 (1 H, t, J = 7.6 Hz, CH – 10), 8.06 (1 H, d, J = 7.2 Hz, CH – 3), 8.14 (2 H, d, J = 8.0 Hz, CH – 6 and 9), 8.48 (1 H, d, J = 7.2 Hz, CH – 12); ^{13}C{^{1}H} NMR ($CDCl_3$) δ = 23.1 (C – 16 and 16'), 23.1 (C – 18 and 18'), 28.7 (C – 17 and 17'), 123.0 (C - 21), 123.5 (C – 6 or 9), 123.6 (C – 20 and 20'), 123.7 (C –6 or 9), 128.4 (C –12), 129.0 (C – 4), 129.5 (C – 5), 129.7 (C – 3), 131.5 (C – 2), 132.3 (C – 11), 132.5 (C – 7), 132.8 (C - 8), 133.0 (C – 13), 135.3 (C – 10), 136.8 (C –

19 and 19'), 148.2 (C – 15), 154.0 (C – 1), 179.8 (C – 14). HRMS (ESI^+): m/z calcd. for $C_{26}H_{25}NO$: 368.2014; found: 368.2015.

N-(4-Chloro-2,6-diisopropylphenyl)-9,10-iminophenanthrenequinone (2).

Phenanthrenequinone (1.0286 g, 4.94 mmol) and aniline (1.30 cm^3, 5.79 mmol) were reacted according to the method to yield (**2**) as a dark green crystalline solid (0.6967 g, 35 %). M.Pt.: 164 – 168 ºC. υ_{max} (cm^{-1}): 3065 (w), 2961 (s), 2926 (m), 2867 (m), 1677 (m, C=O), 1614 (m), 1592 (s, C=N), 1451 (s), 1430 (m), 1295 (s), 1285 (s), 1259 (s), 1233 (s), 759 (s) (C – Cl), 794 (s), 773 (s), 744 (s), 723 (s), 706 (m); ^1H NMR ($CDCl_3$): δ = 1.01 (12 H, d, J = 6.4 Hz, CH_3 – 16 and 16'), 1.13 (6 H, d, J = 6.4 Hz, CH_3 – 18 and 18'), 2.60 (2 H, m, CH – 17 and 17'), 7.12 (2 H, s, CH - 20 and 20'), 7.42 (1 H, t, J = 7.2 Hz, CH – 4), 7.51 (1 H, t, J = 7.2 Hz, CH – 5), 7.65 (1 H, t, J = 7.6 Hz, CH – 11), 7.70 (1 H, J = 7.6 Hz, CH – 10), 7.97 (1 H, d, J = 7.2 Hz, CH – 3), 8.05 (2 H, d, J = 8.0 Hz, CH – 6 and 9), 8.36 (1 H, d, J = 7.6 Hz, CH –12); $^{13}C\{^1H\}$ NMR ($CDCl_3$): δ = 22.8 (C – 16 and 16'), 23.0 (C – 18 and 18'), 28.8 (C – 17 and 17'), 122.9 (C – 7), 123.2 (C –20 and 20'), 123.6 (C – 6 or 9), 123.7 (C – 9 or 6), 128.4 (C – 12), 128.9 (C –8), 129.0 (C – 4), 129.5 (C – 5), 129.6 (C – 3), 132.2 (C – 2), 132.5 (C – 11), 135.2 (C - 13), 135.4 (C –10); HRMS (ESI^+): m/z calcd. for $C_{26}H_{24}ClNO$: 402.1625; found: 402.1621.

N-(4-Bromo-2,6-diisopropylphenyl)-9,10-iminophenanthrenequinone (3).

Phenanthrenequinone (1.3849 g, 6.65 mmol) and aniline (1.60 cm^3, 7.49 mmol) were reacted according to the method to yield (**3**) as a dark black crystalline solid (2.5278 g, 85 %). M.Pt.: 180 – 183 ºC. υ_{max} (cm^{-1}): 2959 (s), 2930 (m), 2869 (m), 1681 (m, C=O), 1614 (m), 1592 (s, C=N), 1462 (m), 1450 (s), 1439 (m), 1423 (m), 1297 (m), 1283 (m), 1275 (m), 1258 (w), 1229 (w), 760 (s), 721 (s); ^1H NMR ($CDCl_3$) δ = 1.07 (6 H, d, J = 6.8 Hz, CH_3 – 16 and 16'), 1.17 (6 H, d, J = 6.4 Hz, CH_3 – 18 and 18'), 2.65 (2 H, m, CH – 17 and 17'), 7.31 (2 H, s, CH – 20 and 20'), 7.44 (1 H, m, CH – 4), 7.55 (1 H, m, CH – 5), 7.69 (1 H, m, CH – 11), 7.74 (1 H, m, CH – 10), 8.02 (1 H, d, J = 7.6 Hz, CH – 3), 8.10 (2 H, d, J = 7.6 Hz, CH – 6 and 9), 8.41 (1 H, d, J = 7.6 Hz, CH – 12); $^{13}C\{^1H\}$ NMR ($CDCl_3$): δ = 22.7 (CH_3 – 16 and 16'), 22.9 (CH_3 – 18 and 18'), 28.7 (C - 17 and 17'), 116.6 (C –21), 123.6 (C – 6 or 9), 123.7 (C – 6 or 9), 126.1 (C – 20 and 20'), 128.4 (C – 12), 129.0 (C – 4), 129.5 (C – 3), 129.6 (C – 5), 132.5 (C – 11), 135.5 (C –10), 136.7 (C –

15), 154.4 (C – 1), 190.0 (C – 14); HRMS (ESI^+): m/z calcd. for $C_{26}H_{24}BrNO$: 446.1120; found: 446.1128.

N-(4-Iodo-2,6-diisopropylphenyl)-9,10-iminophenanthrenequinone (4).

Phenanthrenequinone (1.0245 g, 4.94 mmol) and aniline (2.0 cm^3, 9.26 mmol) were reacted according to the method to yield (**4**) as a dark blue crystalline solid (2.0420 g, 84 %). M.Pt.: 160 – 165 ºC; υ_{max} (cm^{-1}): 3069 (w), 2957 (s), 2926 (m), 2867 (m), 1679 (m, C=O), 1612 (m), 1591 (s, C=N), 1462 (m), 1450 (s), 1297 (s), 1282 (s), 1256 (s), 1228 (m), 761 (s), 721 (s); ^1H NMR ($CDCl_3$) δ = 1.10 (6 H, d, J = 6.8 Hz, CH_3 – 16 and 16'), 1.21 (6 H, d, J = 6.4 Hz, CH_3 – 18 and 18'), 2.65 (2 H, m, CH – 17 and 17'), 7.50 (1 H, m, CH – 4), 7.52 (2 H, s, CH – 20 and 20'), 7.60 (1 H, t, J = 6.8 Hz, CH – 5), 7.74 (1 H, t, J = 7.6 Hz, CH – 11), 7.80 (1 H, t, J = 7.2 Hz, CH – 10), 8.07 (1 H, d, J = 7.6 Hz, CH – 3), 8.15 (2 H, d, J = 7.6 Hz, CH – 6 and 9), 8.45 (1 H, d, J = 7.6 Hz, CH –12); $^{13}C\{^1H\}$ NMR ($CDCl_3$) δ = 22.8 (CH_3 – 16 and 16'), 23.0 (CH_3 – 18 and 18'), 28.7 (CH – 17 and 17'), 87.7 (C – 21), 123.0 (C –20 and 20'), 123.7 (C – 6 or 9), 123.8 (C – 7), 128.5 (C – 8), 129.1 (C –12), 129.6 (C – 2), 129.7 (C – 4), 131.2 (C – 5), 132.2 (C – 3), 132.6 (C – 11), 135.3 (C – 13), 135.5 (C – 10), 135.7 (C – 19 and 19'), 136.7 (C – 15), 148.1 (C – 1), 179.1 (C – 14); HRMS (ESI^+): m/z calcd. for $C_{26}H_{24}INO$: 494.0981; found: 494.0982.

N-(2,4,6-trimethylphenyl)-9,10-iminophenanthrenequinone (5).

Phenanthrenequinone (1.0013 g, 4.80 mmol) and 2,4,6–trimethylaniline (1.00 cm^3, 7.12 mmol) were reacted according to the method to yield (**5**) as a dark green crystalline solid (0.2136 g, 14 %). M.Pt.: 132 – 135 ºC; υ_{max} (cm^{-1}): 2916 (m), 2849 (m), 1675 (m, C=O), 1601 (m), 1590 (s, C=N), 1473 (m), 1450 (s), 1369 (w), 1293 (s), 1277 (s), 1247 (s), 1224 (m), 850 (s), 805 (w), 781 (w), 757 (s), 730 (m), 716 (s), 659 (w): ^1H NMR ($CDCl_3$): δ = 1.97 (6 H, s, CH_3 – 16 and 16'), 2.08 (3 H, s, CH_3 – 20), 6.89 (2 H, s, CH – 18 and 18'), 7.39 (1 H, t, J = 7.6 Hz, CH – 4), 7.49 (1 H, t, J = 7.6 Hz, CH – 5), 7.62 (1 H, m, CH – 11), 7.69 (1 H, m, CH – 10), 8.02 (3 H, m, CH – 3, 6 and 9), 8.42 (1 H, d, J = 7.6 Hz, CH – 12); $^{13}C\{^1H\}$ NMR ($CDCl_3$): δ = 18.2 (C -16 and 16'), 21.0 (C – 20), 122.7 (C – 17 and 17'), 123.6 (C – 6), 123.7 (C – 9), 128.1 (C – 8), 128.3 (C – 12), 128.6 (C – 18 and 18'), 128.9 (C – 4), 129.4 (C – 5), 129.7 (C – 3), 131.1 (C – 7), 132.0 (C – 2),

132.3 (C – 11), 132.7 (C – 13), 135.3 (C – 10), 136.9 (C – 15), 147.9 (C – 1), 180.0 (C – 14); HRMS (ESI^+): m/z calcd. for $C_{23}H_{19}NO$: 326.1545; found: 326.1546.

N-(2,6-dimethylphenyl)-9,10-iminophenanthrenequinone (6).

Phenanthrenequinone (0.6004 g, 2.88 mmol) and 2,6–dimethylaniline (0.68 cm^3, 5.76 mmol) were reacted according to the method to yield (**6**) as a dark blue crystalline solid (535 mg, 60%). M.P.: 75-81°C; υ_{max} (cm^{-1}): 3072 w (Aryl C-H), 2936 w (CH_3), 1677 m (C=O), 1610 w, 1591 s (C=N), 1465 m, 1450 s (C-H def), 1326 w, 1293 m, 1186 w, 1091 m, 1023 m, 939 m, 835 w, 754 s (Aromatic oop), 720 s; ^1H NMR ($CDCl_3$): δ = 1.99 (6H, s, CH_3 – 16,16'), 6.97 (1H, t, J = 7.5Hz, CH-19), 7.09 (2H, d, J=7.5Hz, CH-18,18'), 7.42 (1H, t, J=7.4Hz, CH-4), 7.52 (1H, t, J=7.4Hz, CH-5), 7.66 (1H, t, J=7.7Hz, CH-11), 7.72 (1H, t, J=7.7Hz, CH-10), 8.04 (3H, m, CH-3,6,9), 8.47 (1H, d, J=7.8Hz, CH-12); $^{13}C\{^1H\}$ NMR ($CDCl_3$): δ = 18.2 (C – 16,16'), 122.6 (C - 17,17'), 122.7 (C - 19), 123.5 (C - 6), 123.6 (C - 9), 127.7 (C – 18, 18') 128.2 (C - 12), 128.8 (C - 4), 129.4 (C -5), 129.6 (C - 3), 132.3 (C - 11), 135.5 (C - 10), 150.3 (C - 1), 179.9 (C - 14). HRMS (ESI^+): m/z calcd. for $C_{22}H_{18}NO$: 312.1382; found: 312.1388.

Table 5. Crystal Data and Refinement Parameters for **1-8.**

	1	**2**	**3**	**4**
CCDC Number	1504190	1504191	1504192	1504193
Empirical formula	$C_{26}H_{25}NO$	$C_{26}H_{24}ClNO$	$C_{26}H_{24}BrNO$	$C_{26}H_{24}INO$
Formula weight	367.47	401.91	446.37	493.36
Crystal system	Triclinic	Monoclinic	Monoclinic	Monoclinic
Space Group	$P\bar{1}$	$P2_1/c$	$P2_1/c$	$P2_1/c$
a (Å)	8.4130(6)	8.0689(3)	9.1013(4)	9.2399(5)
b (Å)	9.6517(7)	14.3634(5)	14.0300(6)	14.2091(8)
c (Å)	27.4561(19)	37.0823(11)	16.4292(6)	16.7858(9)
α (°)	86.914(4)	90	90	90
β (°)	83.286(4)	95.1407(19)	91.0340(10)	95.564(2)
γ (°)	65.873(4)	90	90	90
V ($Å^3$)	2020.7(3)	4280.4(3)	2097.52(15)	2193.4(2)
Z	4	8	4	4
Temperature (K)	100	100	100	100
Density (calculated) ($Mg/m^{3)}$	1.208	1.247	1.414	1.494

Absorption coefficient (mm^{-1})	0.560	1.695	1.977	1.476
F(000)	784	1696	920	992
Crystal size	0.11 x 0.09 x 0.03	0.260 x 0.070 x 0.050	0.260 x 0.170 x 0.080	0.230 x 0.130 x 0.090
Theta range for data collection	1.620 to 68.528	2.393 to 68.341	1.909 to 30.058	1.881 to 29.000
Limiting Indices	$-10\leq h\leq 10$	$-9\leq h\leq 8$	$-12\leq h\leq 12$	$-12\leq h\leq 12$
	$-10\leq k\leq 11$	$-17\leq k\leq 17$	$-19\leq k\leq 19$	$-19\leq k\leq 19$
	$-32\leq l\leq 33$	$-44\leq l\leq 44$	$-23\leq l\leq 20$	$-22\leq l\leq 22$
Reflections collected	24243	39019	37924	42398
Independent reflections	7090 [R(int) = 0.0855]	7776 [R(int) = 0.0718]	6151 [R(int) = 0.0374]	5834 [R(int) = 0.0446]
Completeness to theta (%)	95.8	99.5	100.0	100.0
Refinement method	Full-matrix least-squares on F^2	Full-matrix least-squares on F^2	Full-matrix least-squares on F^2	Full-matrix least-squares on F^2
Data / restraints / parameters	7090 / 933 / 876	7776 / 0 / 531	6151 / 0 / 266	5834 / 11 / 266
Goodness-of-fit on F^2	1.026	1.017	1.015	1.082
Final R indices [I>2sigma(I)]	$R_1 = 0.0864$, $wR_2 = 0.2322$	$R_1 = 0.0542$, $wR_2 = 0.1478$	$R_1 = 0.0323$, $wR_2 = 0.0707$	$R_1 = 0.0474$, $wR_2 = 0.1143$

R indices (all data)	R_1 = 0.1852, wR_2 = 0.3012	R_1 = 0.0711, wR_2 = 0.1604	R_1 = 0.0466, wR_2 = 0.0755	R_1 = 0.0623, wR_2 = 0.1200
Largest diff. peak and hole (e.Å^{-3})	0.800 and -0.261	0.643 and -0.673	0.677 and -0.382	0.770 and -1.391

	5	**6**	**7**	**8**
CCDC Number	1504194	1520301	1520302	1504195
Empirical formula	$C_{23}H_{19}NO$	$C_{22}H_{17}NO$	$C_{20}H_{13}NO$	$C_{22}H_{24}O_2$
Formula weight	325.39	311.36	283.31	320.41
Crystal system	Triclinic	Triclinic	Triclinic	Monoclinic
Space Group	$P\bar{1}$	$P\bar{1}$	P1	$P2_1/n$
a (Å)	8.1026(9)	8.5936(11)	5.5249(4)	8.3639(4)
b (Å)	9.4866(11)	9.2038(11)	11.3719(8)	11.6869(6)
c (Å)	12.3706(14)	10.8711(13)	12.4821(9)	18.6543(9)
α (°)	107.042(4)	74.172(5)	108.522(3)	90
β (°)	91.991(5)	73.961(5)	102.295(3)	94.8536(19)
γ (°)	113.538(5)	77.487(5)	100.532(4)	90
V (Å^3)	820.89(16)	785.70(17)	699.50(9)	1816.88(15)

Z	2	2	2	4
Temperature (K)	100	100	100	100
Density (calculated) ($Mg/m^{3)}$	1.316	1.316	1.345	1.171
Absorption coefficient (mm^{-1})	0.080	0.080	0.083	0.073
F(000)	344	328	296	688
Crystal size	0.145 x 0.1 x 0.06	0.38 x 0.13 x 0.04	0.16 x 0.12 x 0.09	0.380 x 0.070 x 0.070
Theta range for data collection	2.784 to 28.416	2.815 to 25.578	3.116 to 25.633	2.058 to 26.000
Limiting Indices	$-10\leq h\leq 10$	$-10\leq h\leq 10$	$-6\leq h\leq 6$	$-10\leq h\leq 10$
	$-12\leq k\leq 12$	$-10\leq k\leq 11$	$-13\leq k\leq 13$	$-14\leq k\leq 14$
	$-16\leq l\leq 16$	$-13\leq l\leq 13$	$-15\leq l\leq 15$	$-23\leq l\leq 21$
Reflections collected	12392	6469	16171	63057
Independent reflections	4110 [R(int) = 0.0851]	2911 [R(int) = 0.0672]	5236 [R(int) = 0.0859]	3573 [R(int) = 0.0548]
Completeness to theta (%)	99.7	98.4	99.6	100.0
Refinement method	Full-matrix least-squares on F^2	Full-matrix least-squares on F^2	Full-matrix least-squares on F^2	Full-matrix least-squares on F^2
Data / restraints / parameters	4110 / 0 / 229	2911 / 0 / 219	5236 / 42 / 362	3573 / 0 / 223

Goodness-of-fit on F^2	0.998	1.013	1.021	1.023
Final R indices [I>2sigma(I)]	R_1 = 0.0611, wR_2 = 0.1249	R_1 = 0.0598, wR_2 = 0.1427	R_1 = 0.0657, wR_2 = 0.1401	R_1 = 0.0465, wR_2 = 0.1173
R indices (all data)	R_1 = 0.1337, wR_2 = 0.1499	R_1 = 0.1290, wR_2 = 0.1783	R_1 = 0.1210, wR_2 = 0.1666	R_1 = 0.0724, wR_2 = 0.1339
Largest diff. peak and hole (e.$Å^{-3}$)	0.242 and -0.267	0.285 and -0.297	0.585 and -0.442	0.273 and -0.160

AUTHOR INFORMATION

Corresponding Author

* Tel: +353-1-8963501. E-mail: bakerrj@tcd.ie; http://chemistry.tcd.ie/staff/academic/bakerrj

Author Contributions

The manuscript was written through contributions of all authors. All authors have given approval to the final version of the manuscript.

ACKNOWLEDGMENT

We thank TCD for funding this work. JAP is grateful to Advanced Research Computing @ Cardiff (ARCCA) for computing facilities.

References

[1] (a) I. Salzmann, G. Heimel, M. Oehzelt, S. Winkler, N. Koch, *Acc. Chem. Res*. **2016**, 49, 370; (b) B. M. Savoie, N. E. Jackson, L. X. Chen, T. J. Marks, M. A. Ratner, *Acc. Chem. Res.* **2014**, 47, 3385; (c) K. Takimiya, I. Osaka, T. Mori, M. Nakano, *Acc. Chem. Res.* **2014**, 47, 1493.

[2] (a) J. Devkota, R. Geng, R. C. Subedi, T. D. Nguyen, *Adv. Funct. Mater.* **2016**, 26, 3881; (b) D. Sun, E. Ehrenfreund,, Z. V. Valy, *Chem. Commun*. **2014**, 50, 1781.

[3] (a) M. Mas-Torrent, C. Rovira, *Chem. Rev.* **2011**, 111, 4833; (b) H. Sirringhaus, *Adv. Mater.* **2014**, 26, 1319; (c) H. Dong, X. Fu, J. Liu, Z. Wang, W. Hu, *Adv. Mater.* **2013**, 25, 6158; (d) C. Wang, H. Dong, W. Hu, Y. Liu, D. Zhu, *Chem. Rev.* **2012**, 112, 2208.

[4] F. Biedermann, H.-J. Schneider, *Chem. Rev.* **2016**, 116, 5216.

[5] (a) O. Takahashi, Y. Kohno, M. Nishio, *Chem. Rev.* **2010**, 110, 6049; (b) M. Nishio, *Phys. Chem. Chem. Phys.* **2011**, 13, 13873; (c) T. J. Mooibroek, P. Gamez, *CrystEngComm*, **2012**, 14, 8462.

[6] C. A. Hunter, J. K. M. Sanders, *J. Amer. Chem. Soc.* **1990**, 112, 5525.

[7] S. E. Wheeler, K.N. Houk, *J. Amer. Chem. Soc.* **2008**, 130, 10854.

[8] (a) A. J. Neel, M. J. Hilton, M. S. Sigman, F. D. Toste, *Nature*, **2017**, 543, 637; (b) J. W. Hwang, P. Li, K.D. Shimiza, *Org. Biomol. Chem.* **2017**, 15, 1554; (c) S. E. Wheeler, J. W. G. Bloom, *J. Phys. Chem. A*, **2014**, 118, 6133; (d) C. R. Martinez, B. L. Iverson, *Chem. Sci.* **2012**, 3, 2191.

[9] (a) G. Cavallo, P. Metrangolo, R. Milani, T. Pilati, A. Priimagi, G. Resnati, G.Terraneo *Chem. Rev.* **2016**, 116, 2478; (b) A. Bauzá, T. J. Mooibroek, A Frontera, *ChemPhysChem*, **2015**, 16, 2496; (c) R. W. Troff, T. Makela, F. Topic, A. Valkonen, K. Raatikainen, K. Rissanen, *Eur. J. Org. Chem.* **2013**, 1617.

[10] For recent reviews see: (a) L. C. Gilday, S. W. Robinson, T. A. Barendt, M. J. Langton, B. R. Mullaney, P. D. Beer, *Chem. Rev*. **2015**, 115, 7118; (b) R. Bishop, *CrystEngComm*. **2015**, 17, 7448; (c) G. Berger, J. Soubhye, F. Meyer, *Polym. Chem.* **2015**, 6, 3559; (d) A. Mukherjee, S. Tothadi, G. R. Desiraju, *Acc. Chem. Res.* **2014**, 47, 2514; (e) A. Priimagi, G. Cavallo, P. Metrangolo, G. Resnati, *Acc. Chem. Res.* **2013**, 46, 2686; (f) F. Meyer, P. Dubois, *CrystEngComm,* **2013**, 15, 3058.

[11] C. B. Aakeröy, S. Panikkatu, P. D. Chopade, J. Desper, *CrystEngComm,* **2013**, 15, 3125.

[12] See for example: (a) F. M. Amombo Noa, S. A. Bourne, H. Su, E. Weber, L. R. Nassimbeni, *Cryst. Growth Des.* **2016**, 16, 4765; (b) S. Tothadi, P. Sanphui, G. R. Desiraju,

Cryst. Growth Des. **2014**, 14, 5293; (c) C. B. Aakeröy, T. K. Wijethunga, M. Abul Haj, J. Desper, C. Moore, *CrystEngComm,* **2014**, 16, 7218; (d) A. Takemura, L. J. McAllister, P. B. Karadakov, N. E. Pridmore, A. C. Whitwood, D. W. Bruce, *CrystEngComm,* **2014**, 16, 4254; (e) T. J. Mooibroek, P. Gamez *CrystEngComm*, **2013**, 15, 1802; (f) T. J. Mooibroek, P. Gamez, *CrystEngComm*, **2013**, 15, 4565; (g) C. B. Aakeröy, P. D. Chopade, C. Ganser, J. Desper, *Chem. Commun*. **2011**, 47, 4688.

[13] (a) S. K. Singh, A. Das, *Phys. Chem. Chem. Phys.* **2015**, 17, 9596; (b) H. R. Khavasi, A. Ghanbarpour, A. A. Tehrani, *CrystEngComm,* **2014**, 16, 749; (c) T. J. Mooibroek, P. Gamez, *CrystEngComm,* **2012**, 14, 1027; (d) T. J. Mooibroek, P. Gamez, J. Reedijk, *CrystEngComm,* **2008**, 10, 1501.

[14] S. Chakraborty, L. Rajput, G. R. Desiraju, *Cryst. Growth Des.* **2014**, 14, 2571.

[15] G. R. Desiraju, R. Parthasarathy, *J. Am. Chem. Soc.* **1989**, 111, 8725.

[16] (a) A. Mukherjee, G. R. Desiraju, *IUCrJ* **2014**, 1, 49; (b) S. Tothadi, S. Joseph,, G. R. Desiraju, *Cryst. Growth Des.* **2013**, 13, 3242.

[17] P. Frøyen, *Phosphorus, Sulfur Silicon Relat. Elem.* **1993**, 81, 37.

[18] (a) A. D. Rae, A. C. Willis, *Z. Kristallogr.* **2003**, 218, 221; (b) S. Y. Matsuzaki, M. Gotoh, A. Kuboyama, *Mol.Cryst.Liq.Cryst.* **1987**, 142, 127; (c) M. Alleaume, R. Darrouy, J. Housty, *Acta Crystallogr.* **1961**, 14, 1202.

[19] L. –K. Liu, T. –I. Ho, C. –S. Hsu, C. –M. Chang, *Acta Crystallogr.* **1987**, C43, 95.

[20] (a) A. Gavezzotti, L. Lo Presti, *Cryst. Growth Des.* **2016**, 16, 2952; (b) R. Taylor *Cryst. Growth Des.* **2016**, 16, 4165.

[21] O. V. Shishkin, *Chem. Phys. Lett.* **2008**, 458, 96.

[22] K. E. Riley, M. Vazquesz, C. Umemura, C. Miller, K.-A. Tran, *Chem. Eur. J.* **2016**, 22, 17690.

[23] S. K. Sing, S. Kumar, A. Das, *Phys. Chem. Chem. Phys.* **2014**, 16, 8819.

[24] T. Clark, M. Hennemann, J. S. Murray, P. Politzer, *J. Mol. Model.* **2007**, 13, 291–296.

[25] P. Politzer, J. S. Murray, *Cryst. Growth Des.* **2015**, 15, 3767.

[26] See for example (a) N. Mohan, C. H. Suresh, *J. Phys. Chem. A,* **2014**, 118, 4315; (b) N. Mohan, C. H. Suresh, A. Kumar, S. R. Gadre, *Phys. Chem. Chem. Phys.* 2013, 15, 18401; (c) Y. Lu, Y. Liu, H. Li, X. Zhu, H. Liu, W. Zhu, *J. Phys. Chem. A* **2012**, 116, 2591; (d) C. Estarellas, A. Frontera, D. Quinonero, P. M. Deya, *Cent. Eur. J. Chem.* **2011**, 9, 25.

[27] M. P. Waller, A. Robertazzi, J. A. Platts, D. E. Hibbs, P. A. Williams, *J. Comput. Chem.* **2006**, 27, 491.

[28] (a) J. J. McKinnon, M. A. Spackman, A. S.; Mitchell, *Acta Crystallogr. Sect. B: Struct. Sci.* **2004**, 60, 627; (b) M. A. Spackman, J. J. McKinnon, *CrystEngComm,* **2002**, 4, 378; (c) *CrystalExplorer* (Version 3.1), S. K. Wolff, D. J. Grimwood, J. J. McKinnon, M. J. Turner, D. Jayatilaka, M. A. Spackman, University of Western Australia, **2012**.

[29] (a) L. A. Cameron, J. W. Ziller, A. F. Heyduk, *Chem. Sci.* **2016**, 7, 1807; (b) G. Szigethy, A. F. Heyduk, *Dalton Trans.* **2012**, 41, 8144; (c) D. M. Togashi, D. E. Nicodem, *Spectrochimica Acta Part A,* **2004**, 60, 3205.

[30] C. Popeney, Z. B. Guan, *Organometallics,* **2005**, 24, 1145.

[31] J. H. Oskam, H. H. Fox, K. B. Yap, D. H. McConville, R. O`Dell, B. J. Lichtenstein, R. R. Schrock, *J. Organomet. Chem.* **1993**, 459, 185.

[32] S. Meiries, S. Nolan, *Synlett.* **2013**, 25, 393.

[33] S. V. Kudrevich, M. G. Galpern, E. A. Luk, J. E. Van Lier, *Can. J. Chem.* **1996**, 74, 508.

[34] Bruker APEX v2012.12-0, Bruker AXS Inc., Madison, Wisconsin, USA.

[35] SADABS (**2014**) Bruker AXS Inc., Madison, Wisconsin, USA; Sheldrick, G. M. University of Göttingen, Germany.

[36] Sheldrick, G.M. (2015). Acta Cryst. A71, 3-8.

[37] Sheldrick, G.M. (2008). Acta Cryst. A64, 112-122.

[38] Dolomanov, O.V., Bourhis, L.J., Gildea, R.J, Howard, J.A.K. & Puschmann, H. (2009), J. Appl. Cryst. 42, 339-341.

[39] Gaussian 09, Revision C.01, M. J. Frisch, G. W. Trucks, H. B. Schlegel, G. E. Scuseria, M. A. Robb, J. R. Cheeseman, G. Scalmani, V. Barone, B. Mennucci, G. A. Petersson, H. Nakatsuji, M. Caricato, X. Li, H. P. Hratchian, A. F. Izmaylov, J. Bloino, G. Zheng, J. L. Sonnenberg, M. Hada, M. Ehara, K. Toyota, R. Fukuda, J. Hasegawa, M. Ishida, T. Nakajima, Y. Honda, O. Kitao, H. Nakai, T. Vreven, J. A. Montgomery, Jr. J. E. Peralta, F. Ogliaro, M. Bearpark, J. J. Heyd, E. Brothers, K. N. Kudin, V. N. Staroverov, T. Keith, R. Kobayashi, J. Normand, K. Raghavachari, A. Rendell, J. C. Burant, S. S. Iyengar, J. Tomasi, M. Cossi, N. Rega, J. M. Millam, M. Klene, J. E. Knox, J. B. Cross, V. Bakken, C. Adamo, J. Jaramillo, R. Gomperts, R. E. Stratmann, O. Yazyev, A. J. Austin, R. Cammi, C. Pomelli, J. W. Ochterski, R.

L. Martin, K. Morokuma, V. G. Zakrzewski, G. A. Voth, P. Salvador, J. J. Dannenberg, S. Dapprich, A. D. Daniels, O. Farkas, J. B. Foresman, J. V. Ortiz, J. Cioslowski,, D. J. Fox, Gaussian, Inc. Wallingford CT, 2010.

[40] Y. Zhao, D. G. Truhlar, *Theor. Chem. Acc.* **2008**, 120, 215.

[41] F. Weigend, R. Ahlrichs, *Phys. Chem. Chem. Phys.* **2005**, 7, 3297.

[42] S. F. Boys, F. Bernardi, *Mol. Phys.* **1970**, 19, 553.

[43] AIMAll (Version 12.06.03), Todd A. Keith, TK Gristmill Software, Overland Park KS, USA, **2012**.